Redox-active tetraruthenium metallacycles: Reversible release of up to eight electrons

Daniel Fink, Bernhard Weibert and Rainer F. Winter*

Fachbereich Chemie, Universität Konstanz, Universitätsstraße 10, D-78453 Konstanz, Germany

Electronic Supplementary Material

Experimental Details

Methods and Materials.

All manipulations were done under purified nitrogen with dry, distilled and nitrogen-saturated solvents. All reagents were purchased from commercial sources and used without further purification. ^{1}H NMR (400 MHz), ^{13}C NMR (101 MHz) and ^{31}P NMR (162 MHz) spectra were measured on a Bruker Avance III 400 spectrometer, and ^{1}H NMR (600 MHz and ^{31}P (243 MHz) NMR spectra on a Bruker AvanceIII 600 spectrometer. Elemental analyses (C, H, N) were performed at in-house facilities on an Elementar Analyzer Vario MICRO Cube of Heraeus. $HRu(CO)Cl(P^{i}Pr_3)_2$,[1] $\{Ru(CO)Cl(P^{i}Pr_3)_2\}_2(\mu\text{-}CH{=}CH\text{-}C_6H_4\text{-}CH{=}CH)$,[2] diphenylamino isophthalic acid[3] and di(4-anisyl)amino isophthalic acid[4] were prepared by literature methods. Mass spectra were recorded on an UHR-ToF Bruker Daltonik (Bremen, Germany) maXis instrument. Detection was done in the positive-ion mode with a 4.5 kV voltage supply. The spectrometer was calibrated with ESI-L Low Concentration Tuning Mix of Agilent prior to every measurement.

Electrochemical and Spectroelectrochemical Measurements.

All electrochemical experiments were performed in a home-built cylindrical vacuum-tight one-compartment cell. A spiral-shaped Pt wire and an Ag wire as the counter and reference electrodes are sealed into glass capillaries that are introduced via Quickfit screws at opposite sides of the cell. A platinum electrode is introduced as the working electrode through the top port via a Teflon screw cap with a suitable fitting. It is polished with first 1 μm and the 0.25 μm diamond paste (Buehler-Wirtz) before measurements. The cell may be attached to a conventional Schlenk line via a side arm equipped with a Teflon screw valve and allows experiments to be performed under an atmosphere of argon with approximately 5 mL of analyte solution. $NBu_4^+ PF_6^-$ (0.25 mM) was used as the supporting electrolyte. Referencing was done with addition of equimolar cobaltocenium hexafluorophosphate as an internal standard to the analyte solution after all data of interest had been acquired. Representative sets of scans were repeated with the added standard. Final referencing was done against the ferrocene/ferrocenium ($Cp_2Fe^{0/+}$) couple with $E_{1/2}$ $Cp_2Co^{+/0}$ = -1330 mV *vs*. $Cp_2Fe^{0/+}$. Electrochemical data were acquired with a computer-controlled BAS potentiostat. The OTTLE cell was also home-built and comprises a Pt-mesh working and counter electrode and a thin silver wire as a pseudo-reference electrode sandwiched between the CaF_2 windows of a conventional liquid IR cell. Its design follows that of Hartl et al.[5] The working electrode is positioned in the center of the spectrometer beam. FT-IR spectra were recorded on a Thermo is10 instrument. UV-Vis/NIR

spectra of the neutral compounds were obtained on a TIDAS fiberoptic diode array spectrometer (combined MCS UV/NIR and PGS NIR instrumentation) from j&m in HELLMA quartz cuvettes with 0.5 cm optical path lengths.

X-Ray diffraction analysis was performed on a STOE IPDS-II diffractometer equipped with a graphite-monochromated radiation source (λ = 0.71073 Å) and an image plate detection system at 100 K. The structure was solved by direct methods (SHELXS-97), completed with difference Fourier syntheses, and refined with full-matrix least-square using SHELXL-97[6] minimizing $\omega(F_0^2\text{-}F_c^2)^2$. Hydrogen atoms were introduces at their calculated positions. Structure plots were made with the Platon program.

Synthesis and characterization

3-H: A solution of 30.4 mg of diphenylamino isophthalic acid (**2-H**, 0.091 mmol) and 13.9 mg (0.100 mmol) of K_2CO_3 in 10 ml of methanol was added to a solution of 100.0 mg (0.091 mmol) of {Ru(CO)Cl(P^iPr_3)$_2$}$_2$(μ-CH=CH-C_6H_4-CH=CH) (**1-Cl**) in 10 ml of CH_2Cl_2. On addition, the initially purple-red colour of the solution of **1-Cl** rapidly changed to pale yellow. The solution was warmed at 50° C for 72 h and then taken to dryness under reduced pressure. The yellow residue was taken up in 40 ml of benzene. Insoluble material was removed by centrifugation, benzene was removed in vacuo and the resulting greenish-yellow residue was washed with three 20 ml portions of n-hexane. Yield: 77 mg (0.028 mmol, 62.3%).

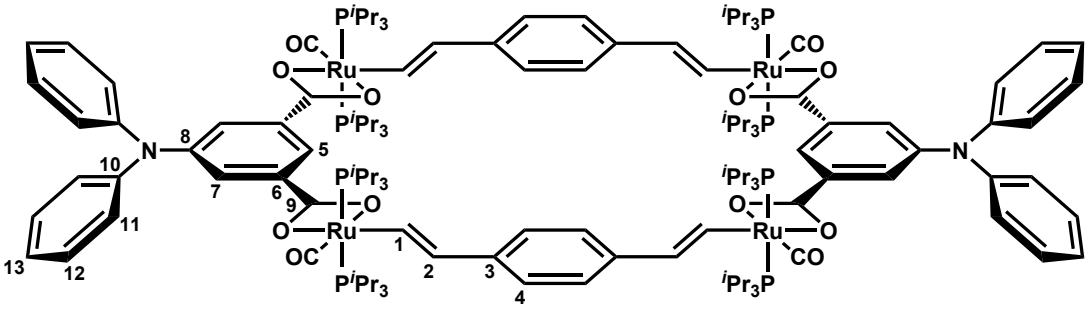

^{1}H NMR (600 MHz, C_6D_6): δ 9.04 (dt, 4H, $^3J_{H,H}$ = 15.3 Hz, $^3J_{H,P}$ = 1.7 Hz, H(1)), 8.89 (t, 2H, $^4J_{H,H}$ = 1.3 Hz, H(5)), 8.22 (d, 4H, $^4J_{H,H}$ = 1.3 Hz, H(7)), 7.50 (s, 8H, H(4)), 6.99 - 6.93 (m, 16H, H(11), H(12)), 6.80 (tt, 4H, $^3J_{H,H}$ = 6.5 Hz, $^4J_{H,H}$ = 1.9 Hz, H(13)), 6.70 (dt, 4H, $^3J_{H,H}$ = 15.3 Hz, $^4J_{H,P}$ = 2.1 Hz, H(2)), 2.35 - 2.24 (m, 24H, P*H*C(CH$_3$)$_2$), 1.31 - 1.18 (m, 144H, PHC(C*H*$_3$)$_2$).

^{31}P{^{1}H} NMR (162 MHz, C_6D_6): δ 38.29 (s, *P*^{i}Pr$_3$).

^{13}C{^{1}H} NMR (151 MHz, C_6D_6): δ 209.7 (t, $^2J_{C,P}$ = 13.8 Hz, Ru*C*O), 176.0 (s, C(9)), 156.4 (t, $^2J_{C,P}$ = 11.6 Hz, C(1)), 148.4 (s, C(8)), 147.6 (s, C(10)), 137.3 (s, C(3)), 135.8 (s, C(6)), 135.5

(s, C(2)), 129.6 (s, C(12)), 126.3 (s, C(7)), 124.8 (s, C(11)), 124.6 (s, C(4)), 123.6 (s, C(5)), 123.6 (s, C(13)), 25.1 (vt, $J_{C,P}$ = 9.3 Hz, P*C*H(CH$_3$)$_2$), 20.0 (s, PCH(*C*H$_3$)$_2$), 19.9 (s, PCH(*C*H$_3$)$_2$).

ESI MS (CH_2Cl_2): m/z = 2717.9927 m/z ([M]$^+$, calculated: 2718.0030), 1358.9969 ([M]$^{2+}$, calculated: 1359.0012).

3-OMe: To a solution of 109.8 mg (0.100 mmol) of **1-Cl** in 20 ml of CH_2Cl_2 a solution of 39.3 mg of dianisylamino isophthalic acid (**2-OMe**) (0.100 mmol) and 15.2 mg (0.110 mmol) of K_2CO_3 in 10 ml of methanol was added, whereupon the solution colour rapidly changed to yellow. The solution was warmed at 50° C for 72 h and then taken to dryness under reduced pressure. The yellow residue was taken up in 25 ml of toluene. Insoluble material was removed by centrifugation, toluene was removed in vacuo and the resulting greenish-yellow residue was washed with three 20 ml portions of n-hexane. Yield: 80 mg (0.028 mmol, 56.4%).

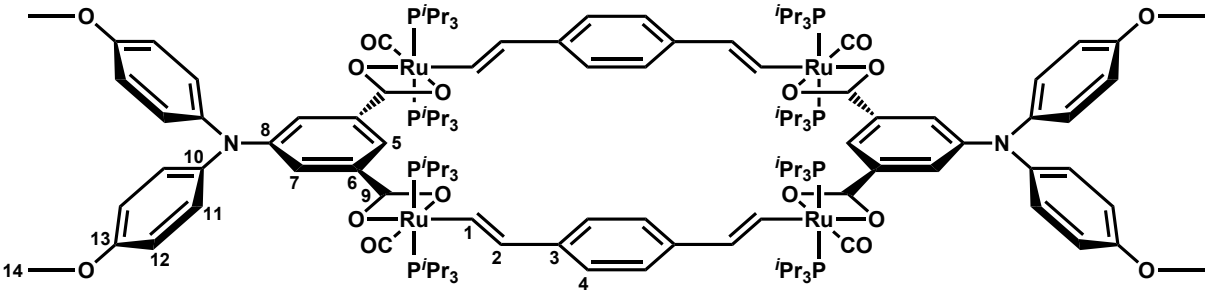

^{1}H NMR (600 MHz, C_6D_6): δ 9.05 (dt, 4H, $^3J_{H,H}$ = 15.3 Hz, $^3J_{H,P}$ = 1.7 Hz, H(1)), 8.80 (t, 2H, $^4J_{H,H}$ = 1.4 Hz, H(5)), 8.16 (d, 4H, $^4J_{H,H}$ = 1.4 Hz, H(7)), 7.50 (s, 8H, H(4)), 6.97 - 6.93 (m, 8H, H(11)), 6.70 (dt, 4H, $^3J_{H,H}$ = 15.3 Hz, $^4J_{H,P}$ = 2.1 Hz, H(2)), 6.67 - 6.63 (m, 8H, H(12)), 3.26 (s, 12H, H(14)) 2.36 - 2.24 (m, 24H, P*H*C(CH$_3$)$_2$), 1.32 - 1.20 (m, 144H, PHC(C*H*$_3$)$_2$).

^{31}P{^{1}H} NMR (162 MHz, C_6D_6): δ 38.33 (s, *P*^{i}Pr$_3$).

^{13}C{^{1}H} NMR (151 MHz, C_6D_6): δ 209.7 (t, $^2J_{C,P}$ = 13.0 Hz, Ru*C*O), 176.4 (s, C(9)), 156.6 (s, C(13)), 156.6 (t, $^2J_{C,P}$ = 11.9 Hz, C(1)), 149.2 (s, C(8)), 140.8 (s, C(10)), 137.3 (s, C(3)), 135.5 (s, C(6)), 135.4 (s, C(2)), 126.8 (s, C(11)), 124.6 (s, C(4)), 123.5 (s, C(7)), 122.0 (s, C(5)), 115.1 (s, C(12)), 54.9 (s, C(14)), 25.1 (vt, $J_{C,P}$ = 9.7 Hz, P*C*H(CH$_3$)$_2$), 20.0 (s, PCH(*C*H$_3$)$_2$), 19.9 (s, PCH(*C*H$_3$)$_2$).

Elemental Analysis: Calc. for $C_{140}H_{218}N_2O_{16}P_8Ru_4$ (2837.35 g/mol): C, 59.26%; H, 7.74%; N, 0.99%. Found: C, 58.65%; H, 7.77%; N, 0.94%.

ESI MS (CH_2Cl_2): m/z = 2838.0410 ($[M]^+$, calculated: 2838.0454), 1419.0192 ($[M]^{2+}$,: calculated: 1419.0224 m/z).

Oxidized samples of **3-H** and **3-OMe** were generated by treatment of the neutral compounds with the appropriate amounts of ferrocenium hexafluorophosphate (**3-H**$^{2+}$, **3-OMe**$^{2+}$), or 1,1'-diacetylferrocenium hexafluoroantimonate (**3-OMe**$^{6+}$).

Single crystals of the benzene solvate **3-OMe**·7 C_6H_6 and the CH_2Cl_2 solvate **3-OMe**·8 CH_2Cl_2 were obtained by layering a saturated solution of **3-OMe** in benzene or CH_2Cl_2, respectively, with methanol. Crystallographic data files have been deposited at the Cambridge Crystallographic Data Centre, 12, Union Road, Cambridge CB2 1EZ, [Fax: + 44 1223/336-033; E-mail deposit@ccdc.cam.ac.] and can be obtained free of charge at www.ccdc.cam.ac.uk/conts/retrieving.html. The deposition numbers are CCDC 1450420 (benzene solvate) and 1450451 (CH_2Cl_2 solvate).

NMR spectra

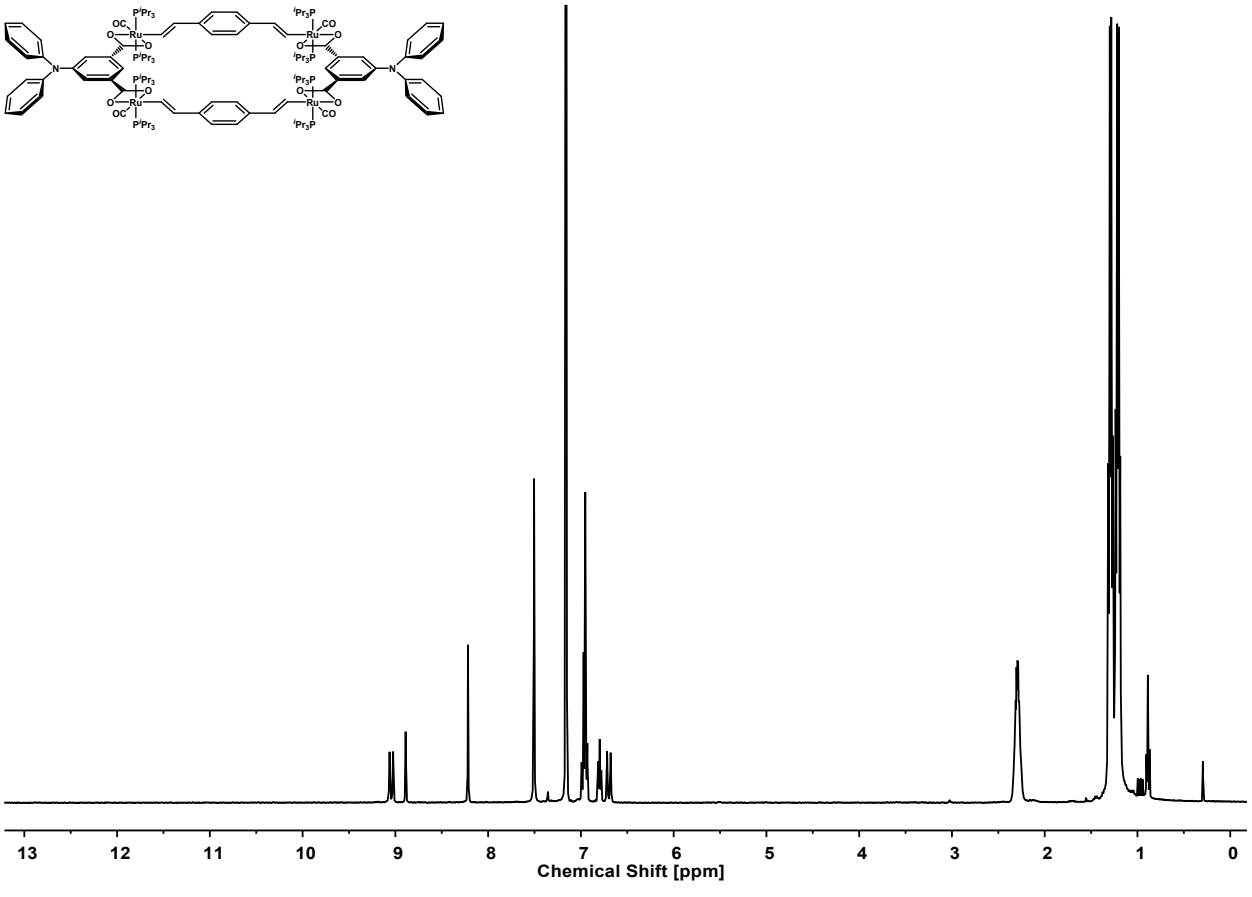

Figure 1. ^{1}H NMR spectrum of macrocycle **3-H**.

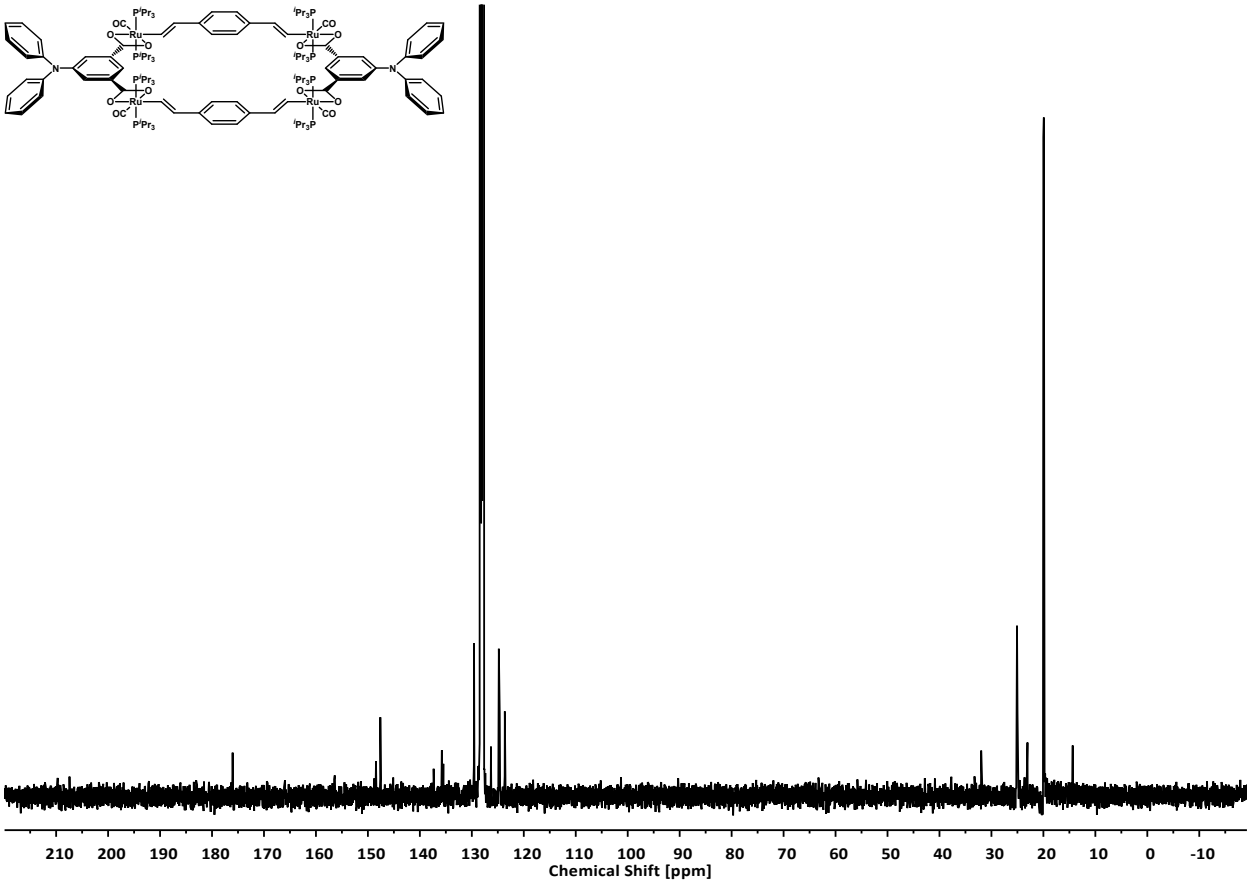

Figure 2. $^{13}C\{^{1}H\}$ NMR spectrum of macrocycle **3-H**.

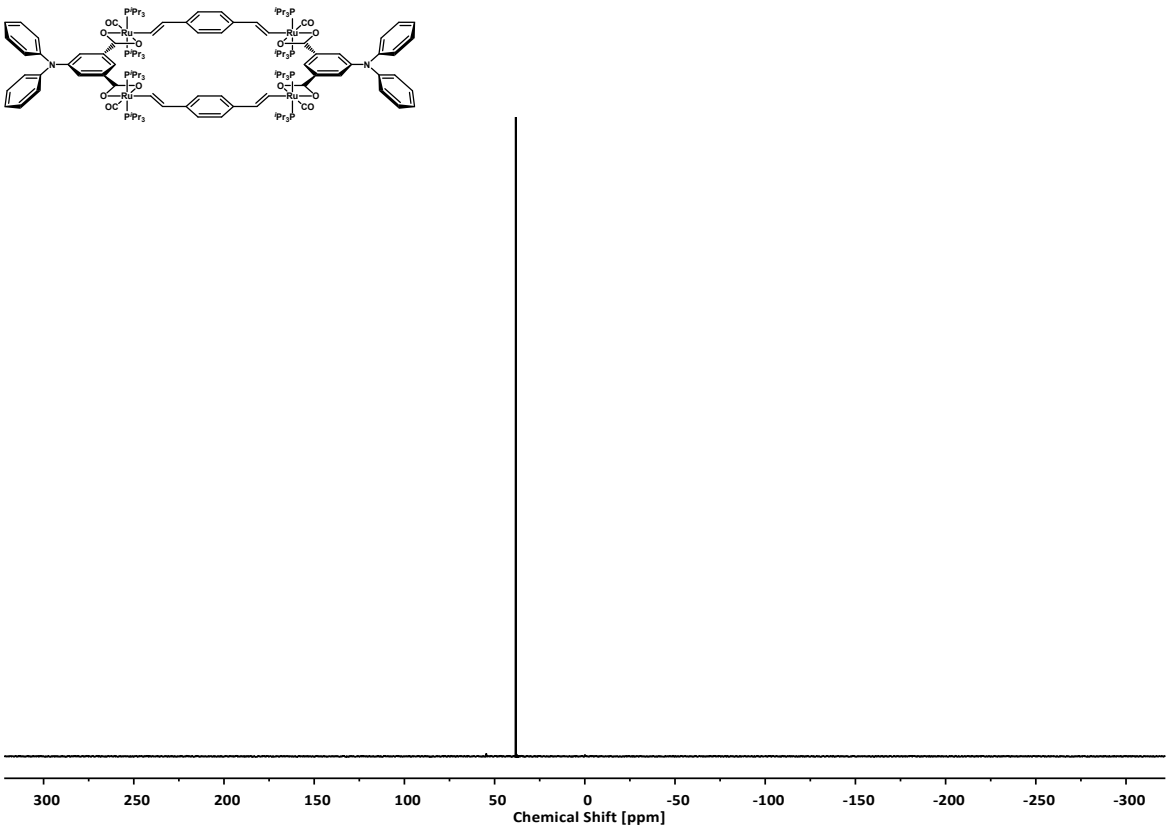

Figure 3. $^{31}P\{^{1}H\}$ NMR spectrum of macrocycle **3-H**.

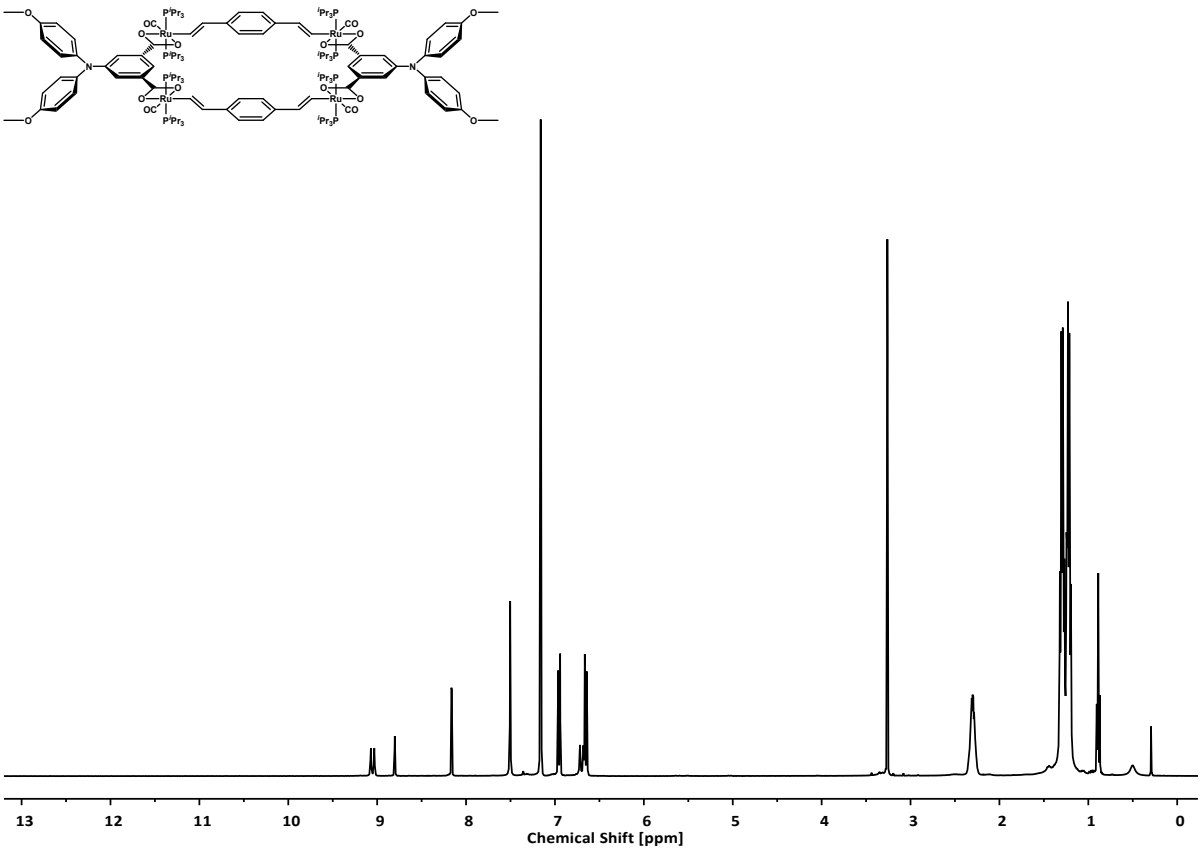

Figure 4. ^{1}H NMR spectrum of macrocycle **3-OMe**.

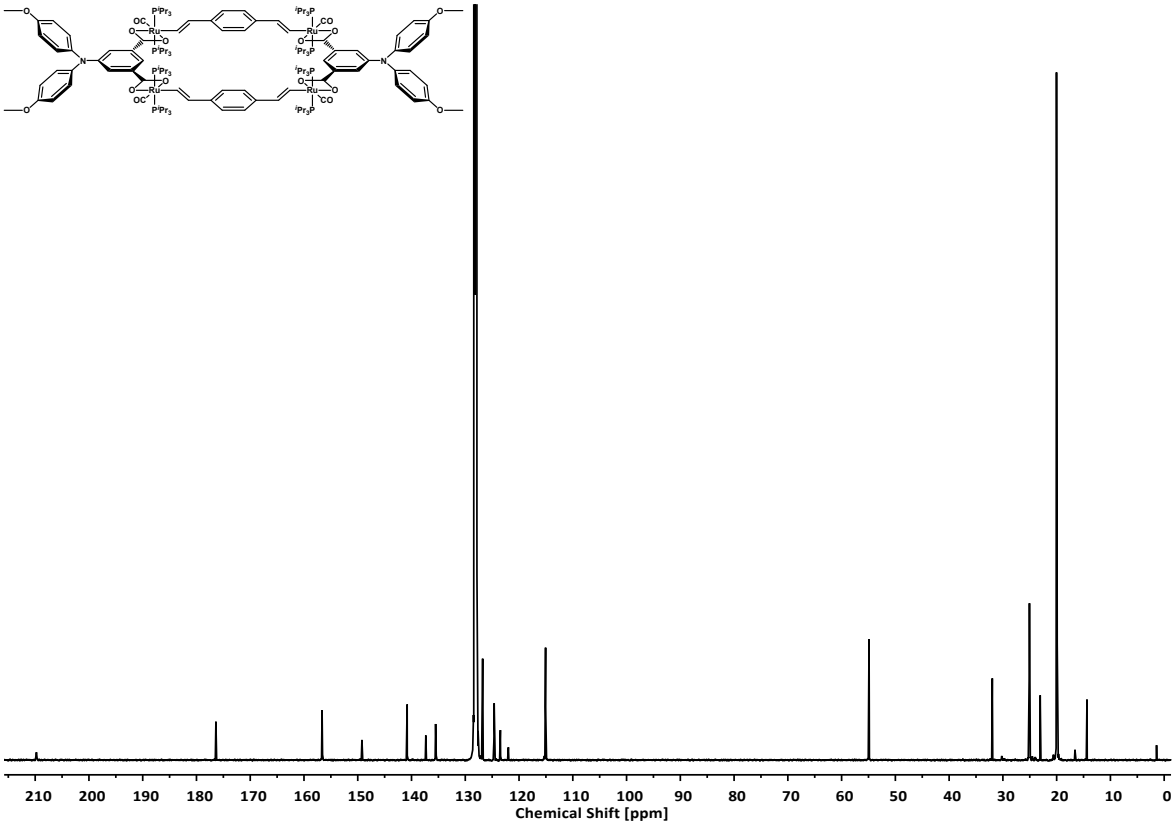

Figure 5. $^{13}C\{^{1}H\}$ NMR spectrum of macrocycle **3-OMe**.

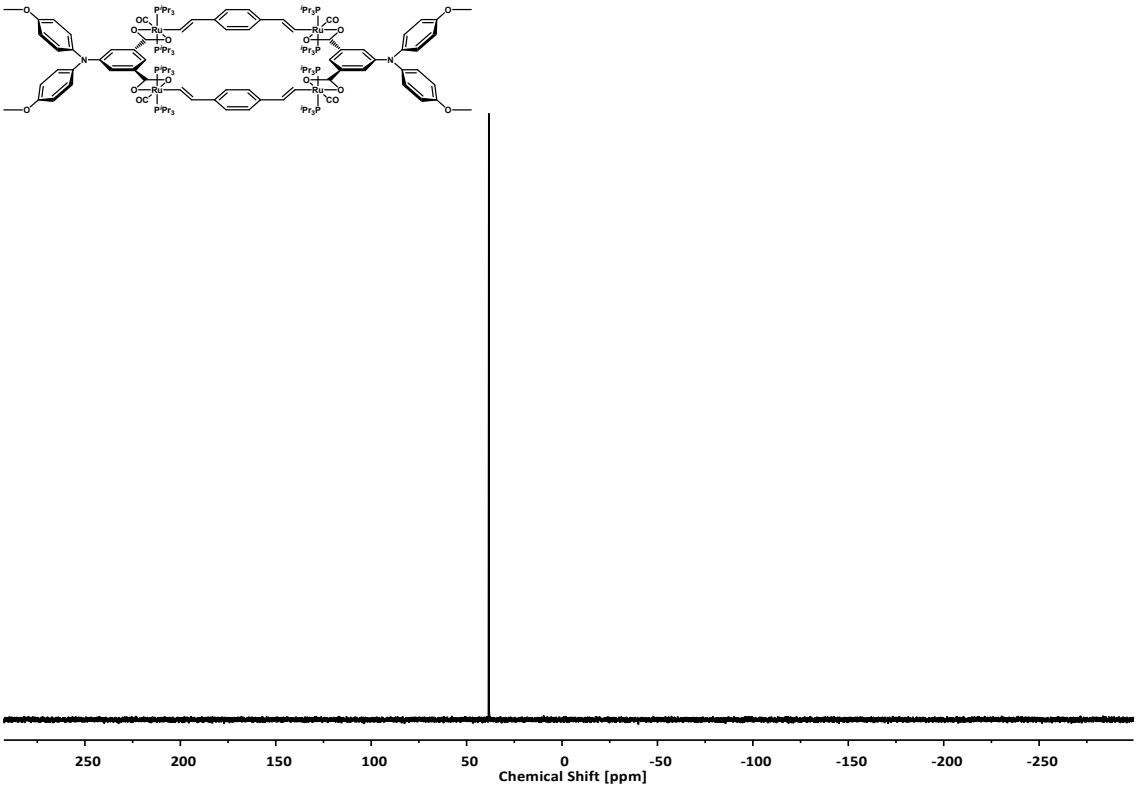

Figure 6. $^{31}P\{^{1}H\}$ NMR spectrum of macrocycle **3-OMe**.

Mass spectrometry

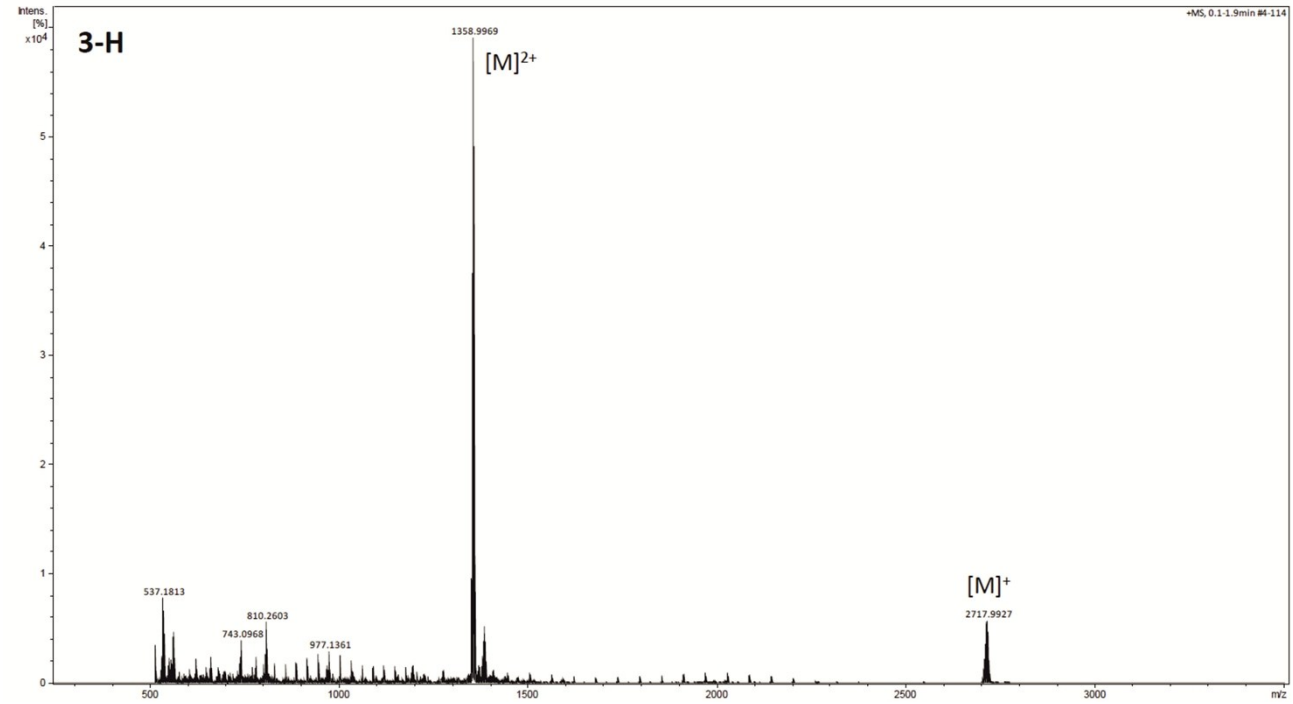

Figure 7. ESI Mass spectrum of macrocycle **3-H**.

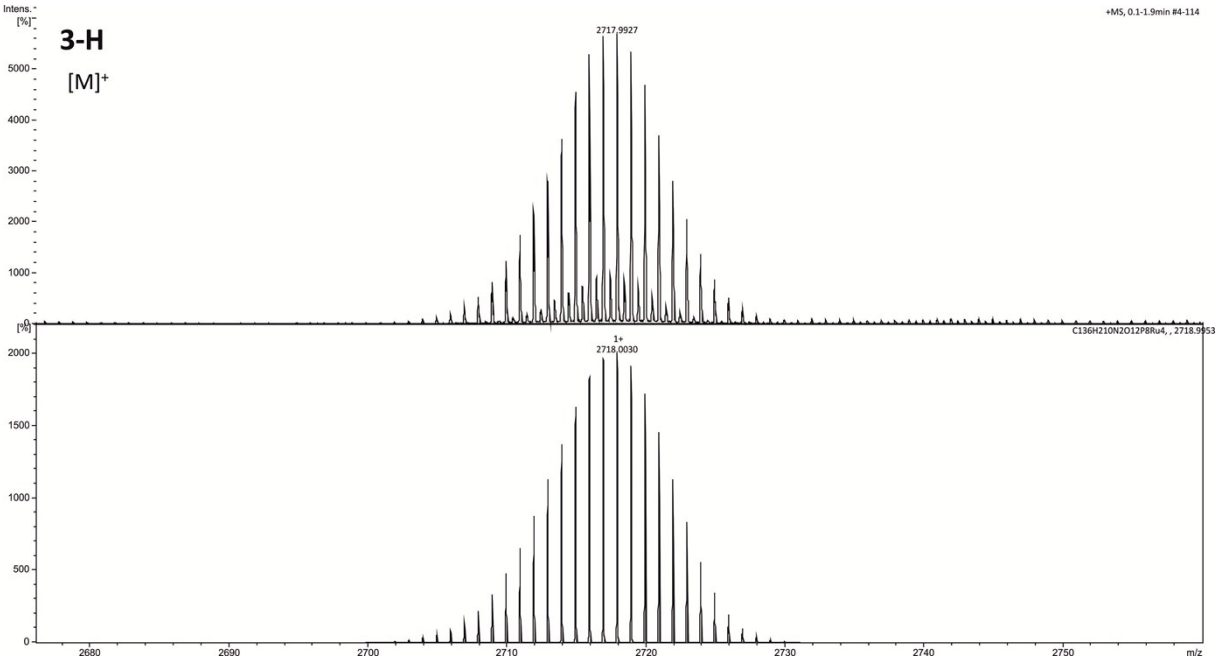

Figure 8. Experimental (top) and simulated (bottom) ESI MS for the peak of the molecule ion M^+ of **3-H**.

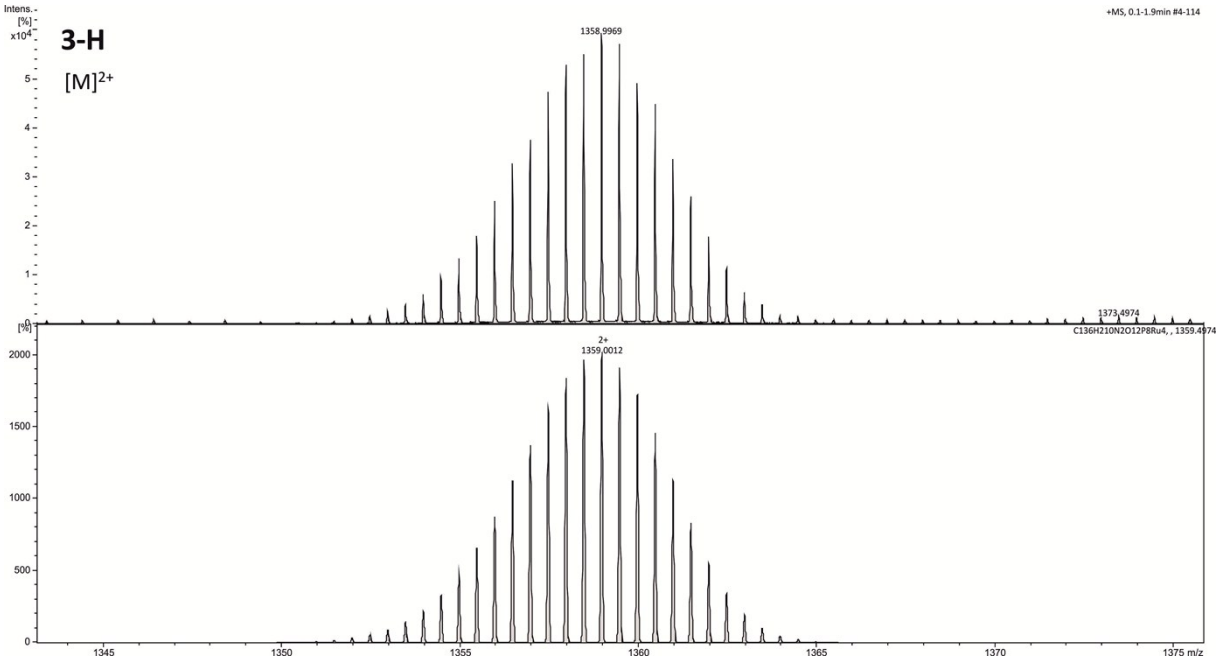

Figure 9. Experimental (top) and simulated (bottom) ESI MS for the peak of the M^{2+} ion of **3-H**.

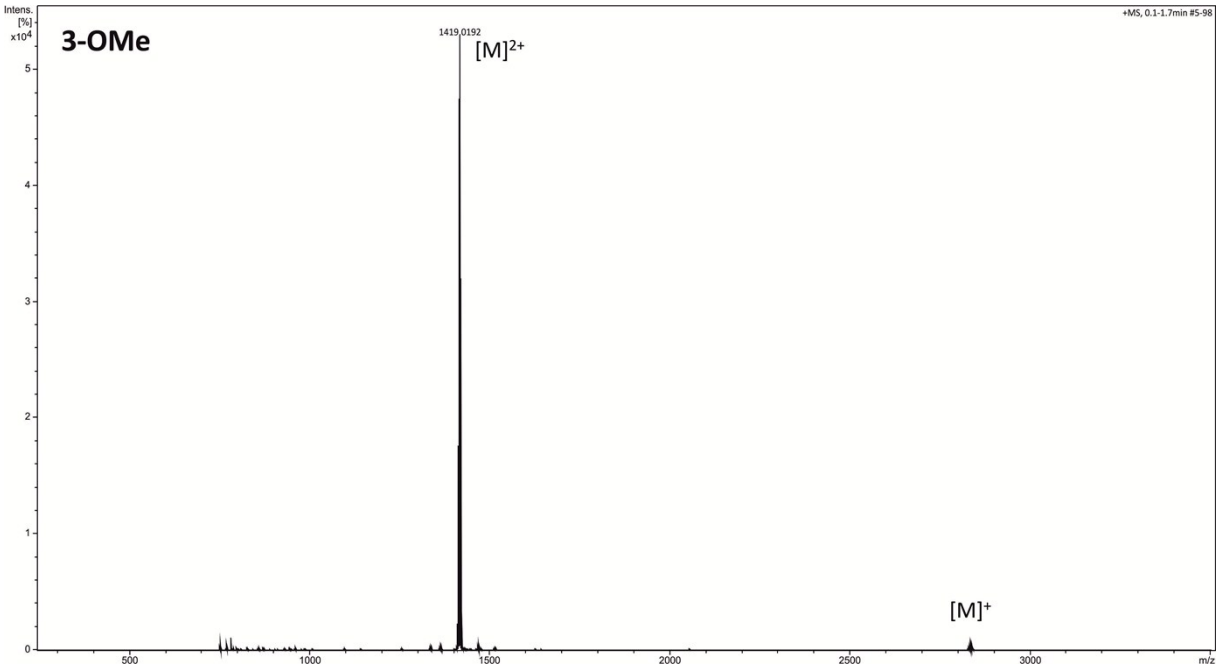

Figure 10. ESI Mass spectrum of macrocycle **3-OMe**.

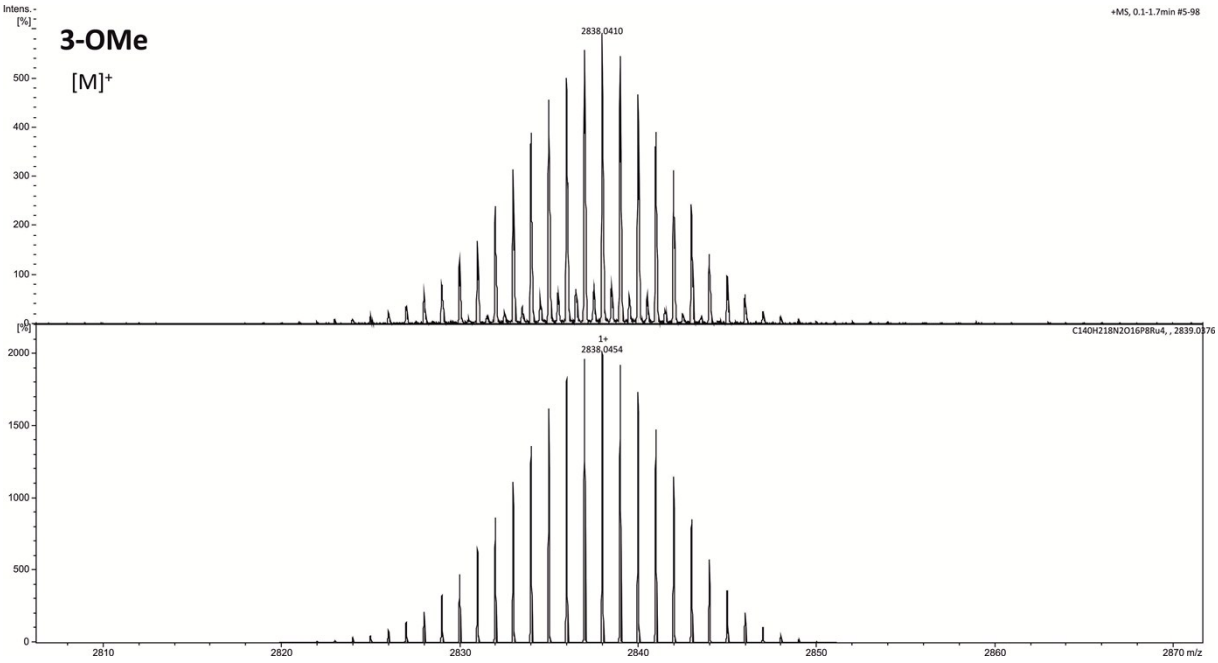

Figure 11. Experimental (top) and simulated (bottom) ESI MS for the peak of the molecule ion of **3-OMe**.

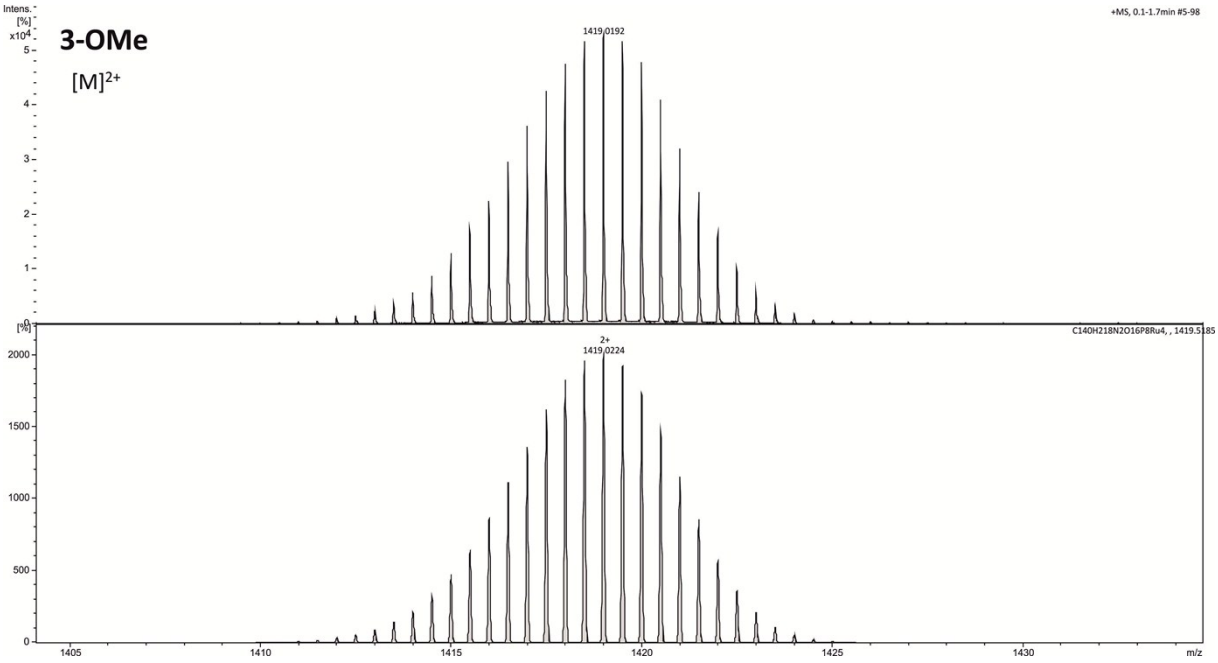

Figure 12. Experimental (top) and simulated (bottom) ESI MS for the peak of the M^{2+} ion of **3-OMe**.

X-ray crystallography

Table 1. Crystal data and structure refinement for 3-OMe·7C_6H_6.

Empirical formula	$C_{182}H_{256}N_2O_{16}P_8Ru_4$
Formula weight	3379.91
Temperature	100(2) K
Wavelength	0.71073 Å
Crystal system	Monoclinic
Space group	*P* 21/*c*
Unit cell dimensions	*a* = 16.1117(13) Å
	b = 26.6027(13) Å β = 100.029(6)°.
	c = 21.6003(14) Å
Volume	9116.7(11) $Å^3$
Z	2
Density (calculated)	1.231 Mg/m^3
Absorption coefficient	0.453 mm^{-1}
F(000)	3572
Crystal size, colour, habit	0.5 x 0.4 x 0.3 mm^3, colourless block
Theta range for data collection	1.494 to 27.032°.
Index ranges	$-20 \le h \le 20$, $-33 \le k \le 33$, $-27 \le l \le 27$
Reflections collected	132362
Independent reflections	19507 [*R*(int) = 0.1944]
Completeness to theta = 25.242°	99.9 %
Absorption correction	Integration
Max. and min. transmission	0.8731 and 0.7023
Refinement method	Full-matrix least-squares on F^2
Data / restraints / parameters	19507 / 0 / 982
Goodness-of-fit on F^2	1.067
Final R indices [I>2sigma(I)]	*R*1 = 0.0970, *wR*2 = 0.2465
R indices (all data)	*R*1 = 0.1305, *wR*2 = 0.2634
Extinction coefficient	0.0037(3)
Largest diff. peak and hole	2.148 and -1.922 e.$Å^{-3}$

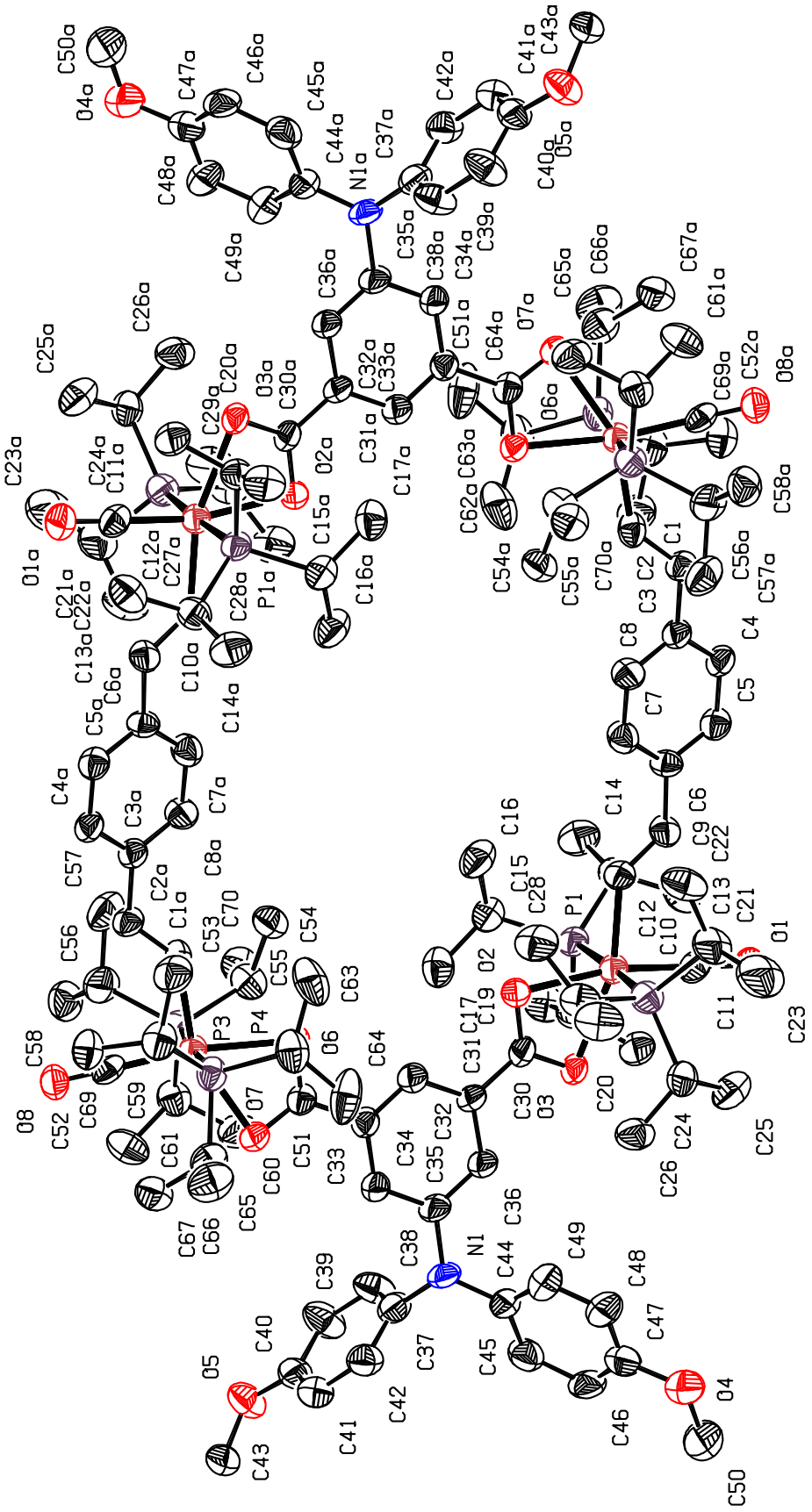

Figure 13. Structure of macrocycle **3-OMe** as the heptabenzene solvate with atom numbering. Benzene solvate molecules and hydrogen atoms have been removed for reasons of clarity. Ellipsoids are drawn at a 50% probability level.

Table 2 Selected bond lengths [Å] and angles [°] for 3-OMe·7C_6H_6.

C(52)-Ru(1)	1.819(8)
O(2)-Ru(2)	2.201(5)
O(3)-Ru(2)	2.267(5)
O(6)-Ru(1)	2.183(5)
O(7)-Ru(1)	2.286(5)
P(1)-Ru(2)	2.402(2)
P(2)-Ru(2)	2.413(2)
P(3)-Ru(1)	2.398(2)
P(4)-Ru(1)	2.404(2)
C(1)-C(2)	1.329(10)
C(1)-Ru(1)#1	2.004(8)
C(2)-C(3)	1.485(10)
C(3)-C(4)	1.389(10)
C(3)-C(8)	1.393(11)
C(4)-C(5)	1.389(10)
C(5)-C(6)	1.388(11)
C(6)-C(7)	1.395(10)
C(6)-C(9)	1.487(10)
C(7)-C(8)	1.394(11)
C(9)-C(10)	1.339(10)
C(10)-Ru(2)	2.014(7)
C(11)-O(1)	1.190(10)
C(11)-Ru(2)	1.777(8)
C(30)-O(2)	1.282(9)
C(30)-O(3)	1.286(8)
C(30)-C(31)	1.471(10)
C(31)-C(32)	1.401(10)
C(31)-C(36)	1.404(10)
C(32)-C(33)	1.376(10)
C(33)-C(34)	1.388(10)
C(33)-C(51)	1.499(10)
C(34)-C(35)	1.390(10)
C(35)-C(36)	1.397(11)
C(35)-N(1)	1.437(9)
C(37)-C(38)	1.368(12)
C(37)-C(42)	1.392(12)
C(37)-N(1)	1.409(10)
C(38)-C(39)	1.398(12)

C(39)-C(40)	1.404(12)
C(40)-C(41)	1.359(12)
C(40)-O(5)	1.362(9)
C(41)-C(42)	1.397(12)
C(43)-O(5)	1.418(10)
C(44)-C(45)	1.389(11)
C(44)-C(49)	1.393(12)
C(44)-N(1)	1.425(10)
C(45)-C(46)	1.464(14)
C(46)-C(47)	1.346(14)
C(47)-C(48)	1.334(14)
C(47)-O(4)	1.458(12)
C(48)-C(49)	1.381(12)
C(50)-O(4)	1.320(13)
C(51)-O(7)	1.263(9)
C(51)-O(6)	1.264(9)
C(52)-O(8)	1.158(9)

C(2)-C(1)-Ru(1)#1	137.1(6)
C(1)-C(2)-C(3)	124.8(7)
C(4)-C(3)-C(8)	116.4(7)
C(4)-C(3)-C(2)	121.3(7)
C(8)-C(3)-C(2)	122.3(7)
C(5)-C(4)-C(3)	122.0(7)
C(6)-C(5)-C(4)	121.6(7)
C(5)-C(6)-C(7)	116.9(7)
C(5)-C(6)-C(9)	118.9(7)
C(7)-C(6)-C(9)	124.1(7)
C(8)-C(7)-C(6)	121.3(7)
C(3)-C(8)-C(7)	121.8(7)
C(10)-C(9)-C(6)	128.4(7)
C(9)-C(10)-Ru(2)	132.7(6)
O(1)-C(11)-Ru(2)	179.4(8)
O(8)-C(52)-Ru(1)	177.5(7)
C(1)#1-Ru(1)-O(6)	96.5(2)
C(52)-Ru(1)-O(7)	112.0(3)
C(1)#1-Ru(1)-O(7)	154.9(2)
O(6)-Ru(1)-O(7)	58.63(18)
C(52)-Ru(1)-P(3)	89.2(2)

C(1)#1-Ru(1)-P(3)	90.9(2)
O(6)-Ru(1)-P(3)	86.11(14)
O(7)-Ru(1)-P(3)	90.85(14)
C(52)-Ru(1)-P(4)	93.2(2)
C(1)#1-Ru(1)-P(4)	89.8(2)
O(6)-Ru(1)-P(4)	91.40(14)
O(7)-Ru(1)-P(4)	87.46(14)
P(3)-Ru(1)-P(4)	177.46(7)
C(52)-Ru(1)-C(51)	140.9(3)
C(1)#1-Ru(1)-C(51)	125.8(3)
O(6)-Ru(1)-C(51)	29.3(2)
O(7)-Ru(1)-C(51)	29.3(2)
P(3)-Ru(1)-C(51)	87.04(17)
P(4)-Ru(1)-C(51)	90.56(17)
C(11)-Ru(2)-C(10)	89.0(3)
C(11)-Ru(2)-O(2)	168.3(3)
C(10)-Ru(2)-O(2)	102.3(3)
C(11)-Ru(2)-O(3)	109.4(3)
C(10)-Ru(2)-O(3)	161.6(2)
O(2)-Ru(2)-O(3)	59.32(17)
C(11)-Ru(2)-P(1)	93.4(3)
C(10)-Ru(2)-P(1)	90.3(2)
O(2)-Ru(2)-P(1)	89.67(15)
O(3)-Ru(2)-P(1)	88.97(14)
C(11)-Ru(2)-P(2)	90.0(3)
C(10)-Ru(2)-P(2)	90.3(2)
O(2)-Ru(2)-P(2)	86.84(15)
O(3)-Ru(2)-P(2)	89.34(14)
P(1)-Ru(2)-P(2)	176.51(8)
C(11)-Ru(2)-C(30)	139.0(3)
C(10)-Ru(2)-C(30)	131.9(3)
O(2)-Ru(2)-C(30)	29.6(2)
O(3)-Ru(2)-C(30)	29.75(19)
P(1)-Ru(2)-C(30)	90.41(18)
P(2)-Ru(2)-C(30)	86.60(18)

Symmetry transformations used to generate equivalent atoms: #1 -x+1,-y+1,-z+1

Table 3. Crystal data and structure refinement for 3-OMe·8CH_2Cl_2.

Empirical formula	$C_{148}H_{234}Cl_{16}N_2O_{16}P_8Ru_4$	
Formula weight	3516.60	
Temperature	100(2) K	
Wavelength	0.71073 Å	
Crystal system	Triclinic	
Space group	P-1	
Unit cell dimensions	a = 11.6168(19) Å	α = 94.410(12)°.
	b = 16.816(2) Å	β = 99.289(12)°.
	c = 23.594(4) Å	γ = 107.587(12)°.
Volume	4297.0(12) $Å^3$	
Z	1	
Density (calculated)	1.359 Mg/m^3	
Absorption coefficient	0.724 mm^{-1}	
F(000)	1832	
Crystal size, colour, habit	0.4 x 0.3 x 0.1 mm^3, yellow plate	
Theta range for data collection	1.651 to 26.028°.	
Index ranges	$-14 \le h \le 14$, $-20 \le k \le 19$, $-29 \le l \le 29$	
Reflections collected	58713	
Independent reflections	16746 [R(int) = 0.2398]	
Completeness to theta = 25.242°	99.9 %	
Absorption correction	Integration	
Max. and min. transmission	0.9823 and 0.8354	
Refinement method	Full-matrix least-squares on F^2	
Data / restraints / parameters	16746 / 0 / 900	
Goodness-of-fit on F^2	0.981	
Final R indices [I>2sigma(I)]	$R1$ = 0.0951, $wR2$ = 0.2303	
R indices (all data)	$R1$ = 0.1538, $wR2$ = 0.2646	
Extinction coefficient	n/a	
Largest diff. peak and hole	1.056 and -1.347 $e.Å^{-3}$	

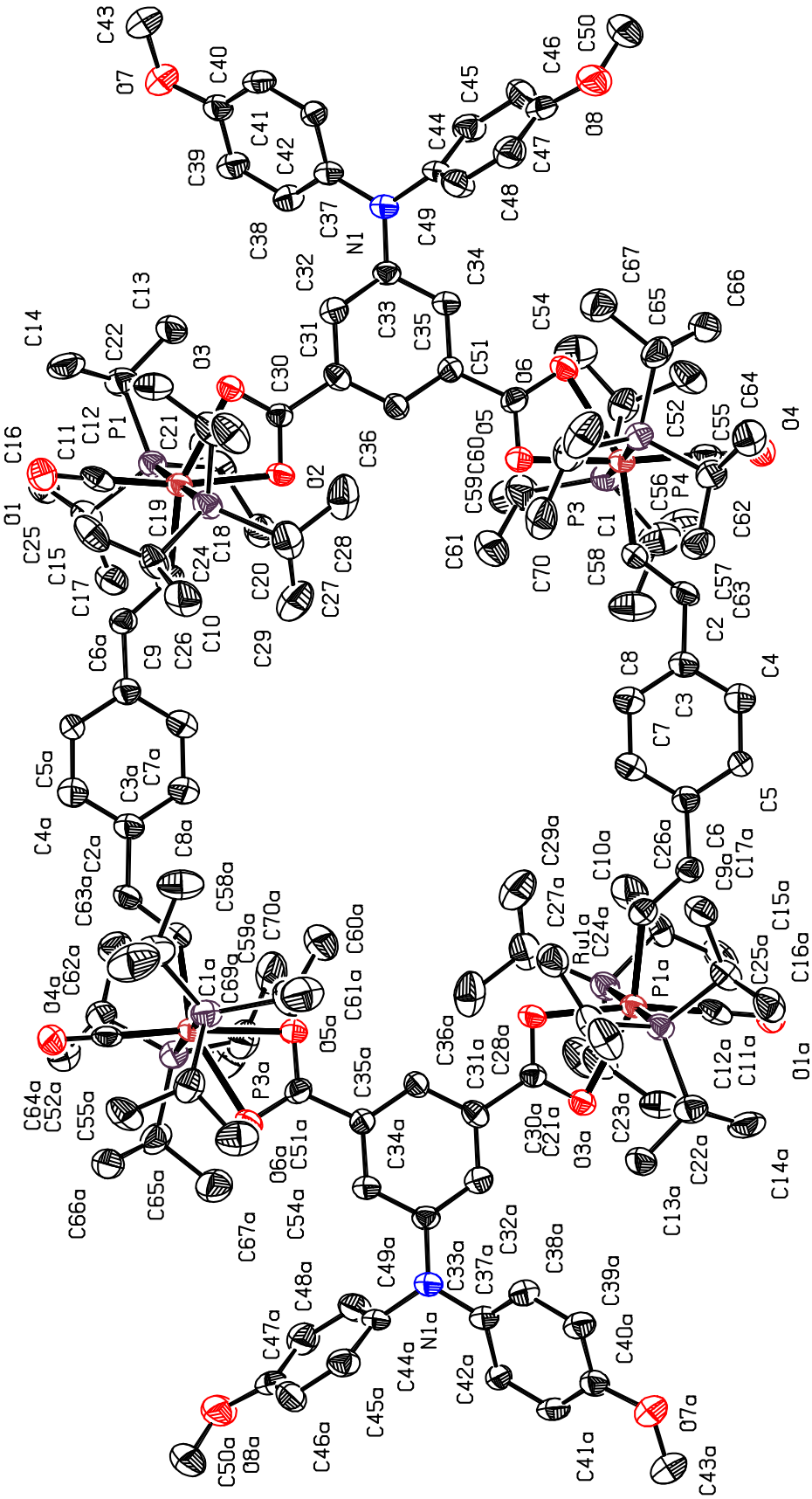

Figure 14. Structure of macrocycle **3-OMe** as the octakis CH_2Cl_2 solvate with atom numbering. Solvate molecules and hydrogen atoms have been removed for reasons of clarity. Ellipsoids are drawn at a 50% probability level.

Table 4. Selected bond lengths [Å] and angles [°] for 3-OMe·8CH_2Cl_2.

Ru(1)-C(11)	1.774(10)
Ru(1)-C(10)	2.009(8)
Ru(1)-O(2)	2.207(6)
Ru(1)-O(3)	2.300(5)
Ru(1)-P(1)	2.405(2)
Ru(1)-P(2)	2.408(2)
Ru(1)-C(30)	2.592(8)
Ru(2)-C(52)	1.795(9)
Ru(2)-C(1)	2.024(8)
Ru(2)-O(5)	2.186(6)
Ru(2)-O(6)	2.305(6)
Ru(2)-P(4)	2.400(3)
Ru(2)-P(3)	2.411(3)
N(1)-C(33)	1.400(10)
N(1)-C(37)	1.421(11)
N(1)-C(44)	1.446(11)
O(1)-C(11)	1.198(11)
O(2)-C(30)	1.261(9)
O(3)-C(30)	1.260(9)
O(4)-C(52)	1.172(10)
O(5)-C(51)	1.275(10)
O(6)-C(51)	1.266(10)
O(7)-C(40)	1.379(11)
O(7)-C(43)	1.393(13)
O(8)-C(47)	1.376(12)
O(8)-C(50)	1.428(14)
C(1)-C(2)	1.331(12)
C(2)-C(3)	1.492(11)
C(3)-C(4)	1.396(13)
C(3)-C(8)	1.400(13)
C(4)-C(5)	1.377(12)
C(5)-C(6)	1.381(12)
C(6)-C(7)	1.378(13)
C(6)-C(9)#1	1.483(11)
C(7)-C(8)	1.401(13)
C(9)-C(10)	1.343(11)
C(9)-C(6)#1	1.483(11)
C(30)-C(31)	1.483(11)

C(31)-C(36)	1.390(12)
C(31)-C(32)	1.396(11)
C(32)-C(33)	1.381(11)
C(33)-C(34)	1.411(12)
C(34)-C(35)	1.398(11)
C(35)-C(36)	1.391(11)
C(35)-C(51)	1.493(11)
C(37)-C(38)	1.384(12)
C(37)-C(42)	1.409(11)
C(38)-C(39)	1.403(13)
C(39)-C(40)	1.390(12)
C(40)-C(41)	1.376(13)
C(41)-C(42)	1.390(12)
C(44)-C(49)	1.365(13)
C(44)-C(45)	1.371(12)
C(45)-C(46)	1.397(13)
C(46)-C(47)	1.388(15)
C(47)-C(48)	1.396(14)
C(48)-C(49)	1.384(13)

C(11)-Ru(1)-C(10)	90.4(4)
C(11)-Ru(1)-O(2)	170.4(3)
C(10)-Ru(1)-O(2)	99.1(3)
C(11)-Ru(1)-O(3)	112.4(3)
C(10)-Ru(1)-O(3)	157.1(3)
O(2)-Ru(1)-O(3)	58.12(19)
C(11)-Ru(1)-P(1)	89.3(3)
C(10)-Ru(1)-P(1)	91.1(2)
O(2)-Ru(1)-P(1)	88.86(16)
O(3)-Ru(1)-P(1)	89.79(15)
C(11)-Ru(1)-P(2)	91.4(3)
C(10)-Ru(1)-P(2)	89.4(2)
O(2)-Ru(1)-P(2)	90.29(16)
O(3)-Ru(1)-P(2)	89.43(15)
P(1)-Ru(1)-P(2)	179.07(8)
C(11)-Ru(1)-C(30)	141.4(3)
C(10)-Ru(1)-C(30)	128.1(3)
O(2)-Ru(1)-C(30)	29.1(2)
O(3)-Ru(1)-C(30)	29.1(2)

P(1)-Ru(1)-C(30)	88.12(18)
P(2)-Ru(1)-C(30)	90.96(18)
C(52)-Ru(2)-C(1)	88.1(3)
C(52)-Ru(2)-O(5)	174.4(3)
C(1)-Ru(2)-O(5)	97.4(3)
C(52)-Ru(2)-O(6)	116.2(3)
C(1)-Ru(2)-O(6)	155.7(3)
O(5)-Ru(2)-O(6)	58.35(19)
C(52)-Ru(2)-P(4)	88.7(3)
C(1)-Ru(2)-P(4)	93.8(3)
O(5)-Ru(2)-P(4)	89.93(17)
O(6)-Ru(2)-P(4)	88.93(16)
C(52)-Ru(2)-P(3)	89.9(3)
C(1)-Ru(2)-P(3)	90.6(3)
O(5)-Ru(2)-P(3)	90.98(18)
O(6)-Ru(2)-P(3)	87.69(16)
P(4)-Ru(2)-P(3)	175.38(8)
C(33)-N(1)-C(37)	122.3(7)
C(33)-N(1)-C(44)	118.5(7)
C(37)-N(1)-C(44)	118.5(6)
C(2)-C(1)-Ru(2)	134.4(6)
C(1)-C(2)-C(3)	125.8(8)
C(4)-C(3)-C(8)	116.5(8)
C(4)-C(3)-C(2)	119.2(8)
C(8)-C(3)-C(2)	124.3(8)
C(5)-C(4)-C(3)	121.4(9)
C(4)-C(5)-C(6)	122.3(8)
C(5)-C(6)-C(7)	117.2(8)
C(5)-C(6)-C(9)#1	119.3(8)
C(7)-C(6)-C(9)#1	123.6(8)
C(6)-C(7)-C(8)	121.4(9)
C(7)-C(8)-C(3)	121.0(9)
C(10)-C(9)-C(6)#1	127.8(8)
C(9)-C(10)-Ru(1)	134.7(7)
O(1)-C(11)-Ru(1)	178.1(7)
O(3)-C(30)-O(2)	120.7(7)

Symmetry transformations used to generate equivalent atoms: #1 -x+1,-y+1,-z+1

Cyclic voltammetry

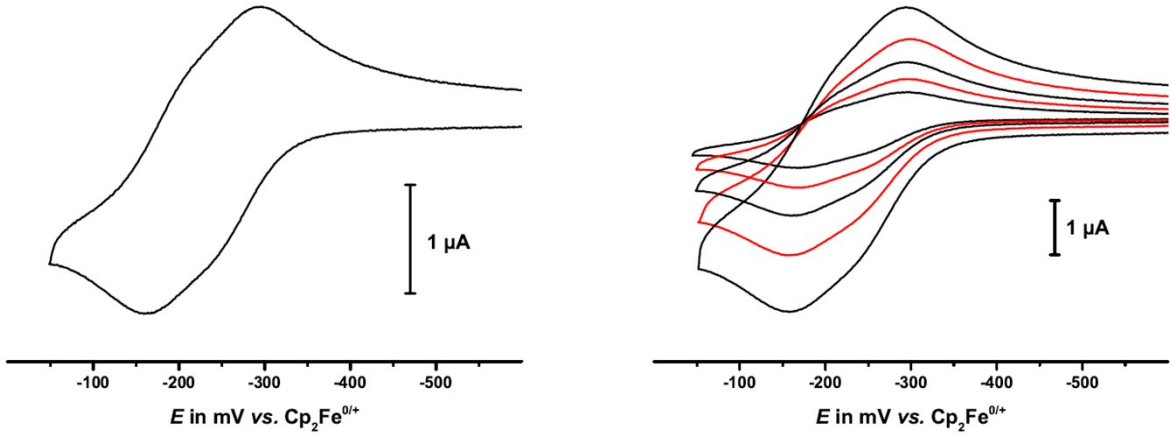

Figure 15. Cyclic voltammograms (v = 0.1 V/s) (left) and at v = 0.025, 0.050, 0.10, 0.20 and 0.40 V/s in CH_2Cl_2/NBu_4PF_6, r. t. for the first composite wave of macrocycle **3-H**.

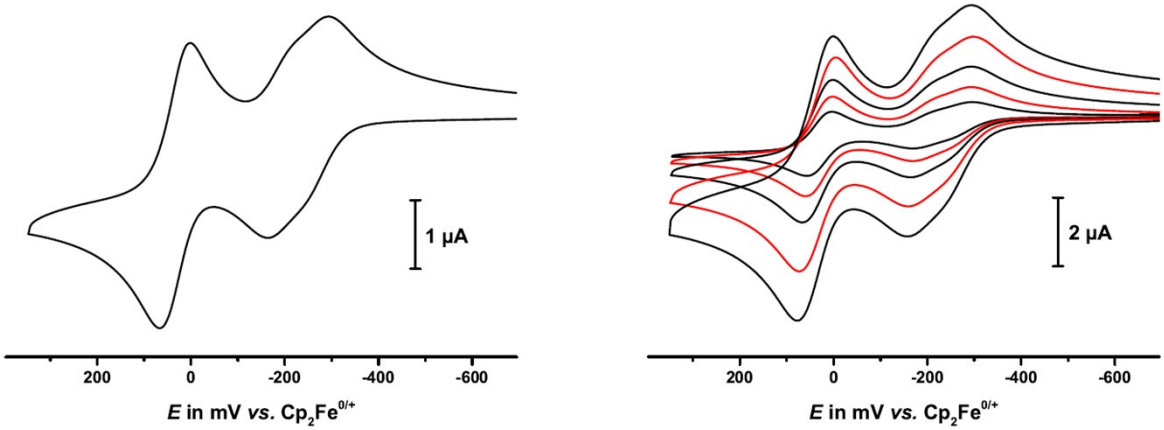

Figure 16. Cyclic voltammograms (**v** = 0.1 V/s) (left) and at v = 0.025, 0.050, 0.10, 0.20 and 0.40 V/s in CH_2Cl_2/NBu_4PF_6, r. t. for the first two composite waves of macrocycle **3-H**.

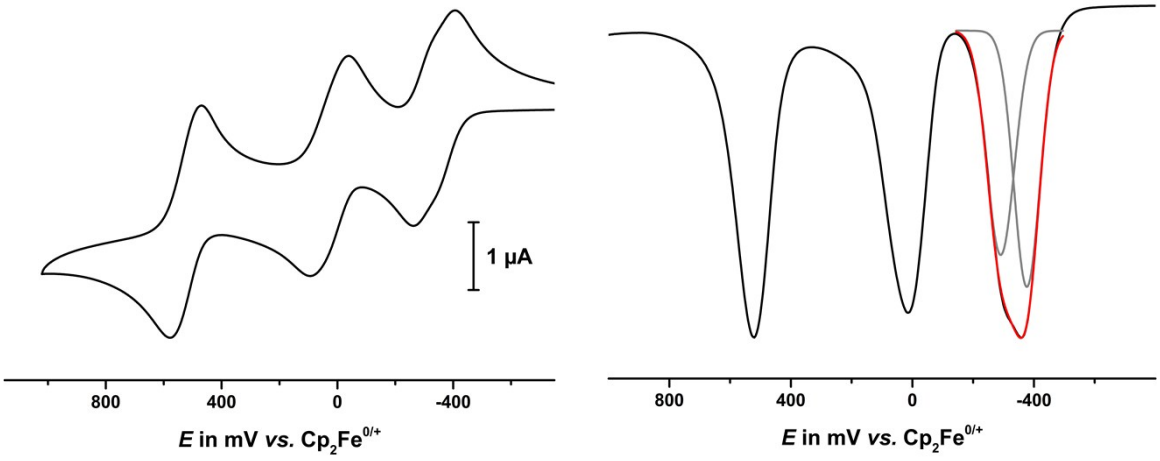

Figure 17. Cyclic voltammogram (v = 0.1 V/s) (left) and square wave voltammogram with deconvolution of the first composite peak (right) in $CH_2Cl_2/NBu_4B\{C_6H_3(CF_3)_2\text{-}3,5\}_4$, r. t. of macrocycle **3-H**.

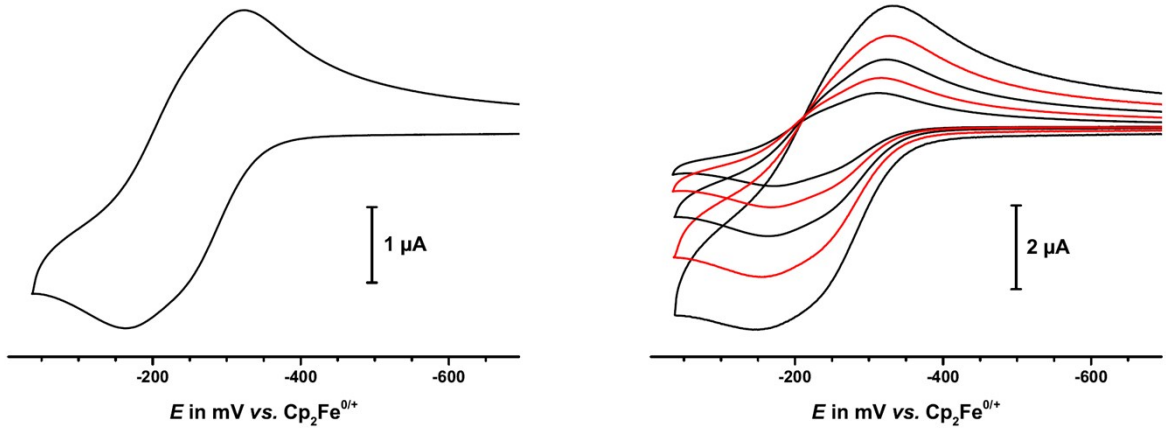

Figure 18. Cyclic voltammograms (v = 0.1 V/s) (left) and at v = 0.025, 0.050, 0.10, 0.20 and 0.40 V/s in CH_2Cl_2/NBu_4PF_6, r. t. for the first composite wave of macrocycle **3-OMe**.

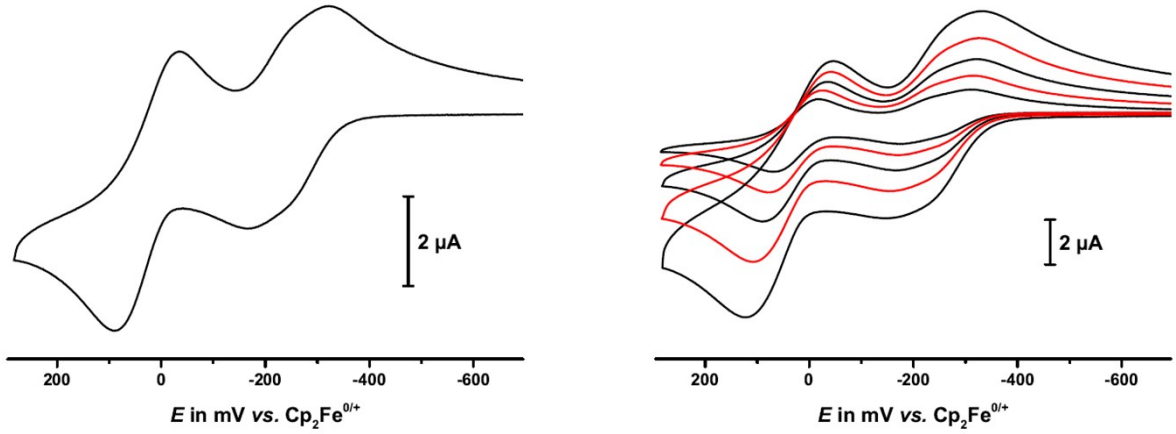

Figure 19. Cyclic voltammograms (v = 0.1 V/s) (left) and at v = 0.025, 0.050, 0.10, 0.20 and 0.40 V/s in CH_2Cl_2/NBu_4PF_6, r. t. for the first two composite waves of macrocycle **3-OMe**.

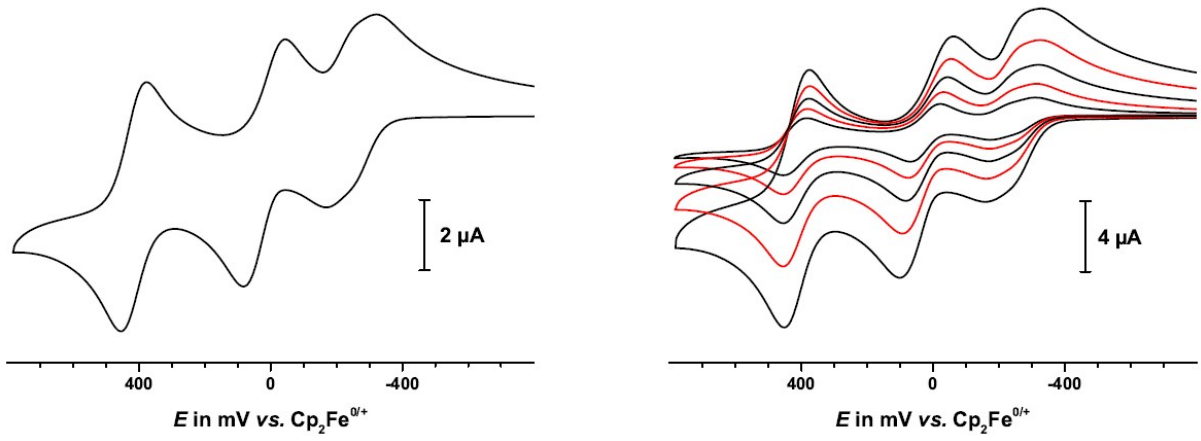

Figure 20. Cyclic voltammograms (v = 0.1 V/s) (left) and at v = 0.025, 0.050, 0.10, 0.20 and 0.40 V/s in CH_2Cl_2/NBu_4PF_6, r. t. for the first three composite waves of macrocycle **3-OMe**.

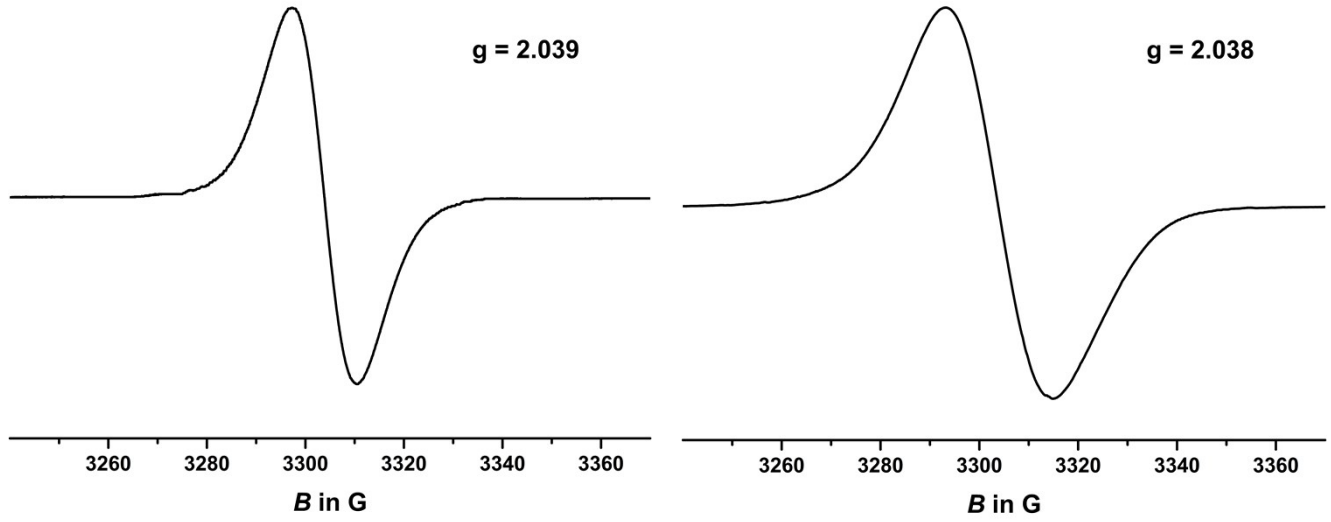

Figure 21. EPR spectrum of **3-H**$^{2+}$ at r. t. (left) and at 123 K (right).

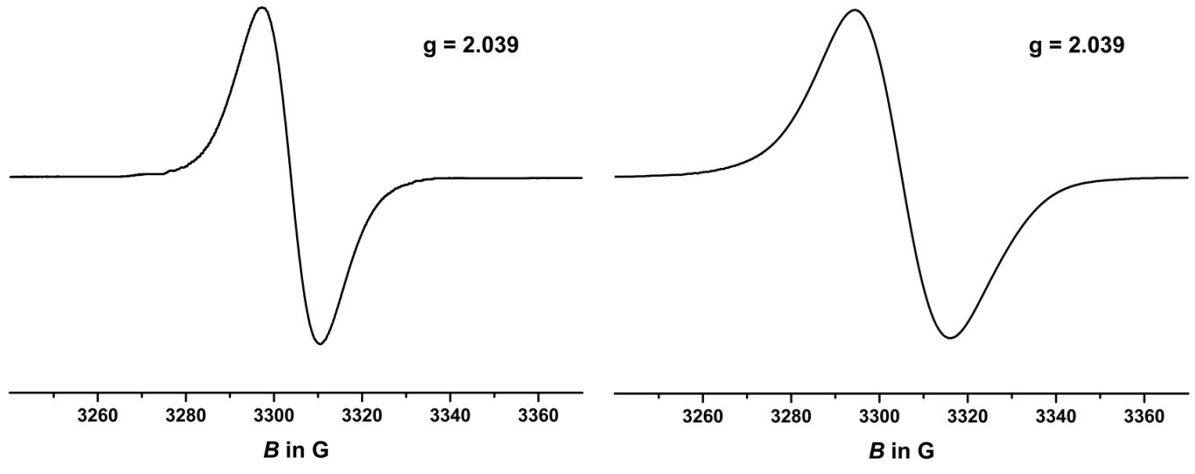

Figure 22. EPR spectrum of **3-OMe**$^{2+}$ at r. t. (left) and at 123 K (right).

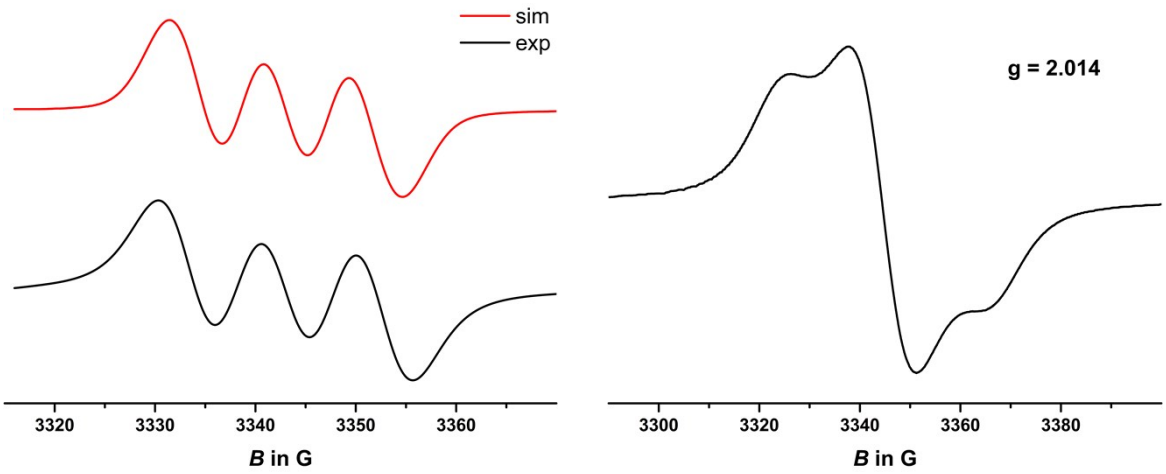

Figure 23. EPR spectrum of **3-OMe**$^{6+}$ in CH_2Cl_2 at r. t. (left) and at 123 K (right).

IR spectroelectrochemistry

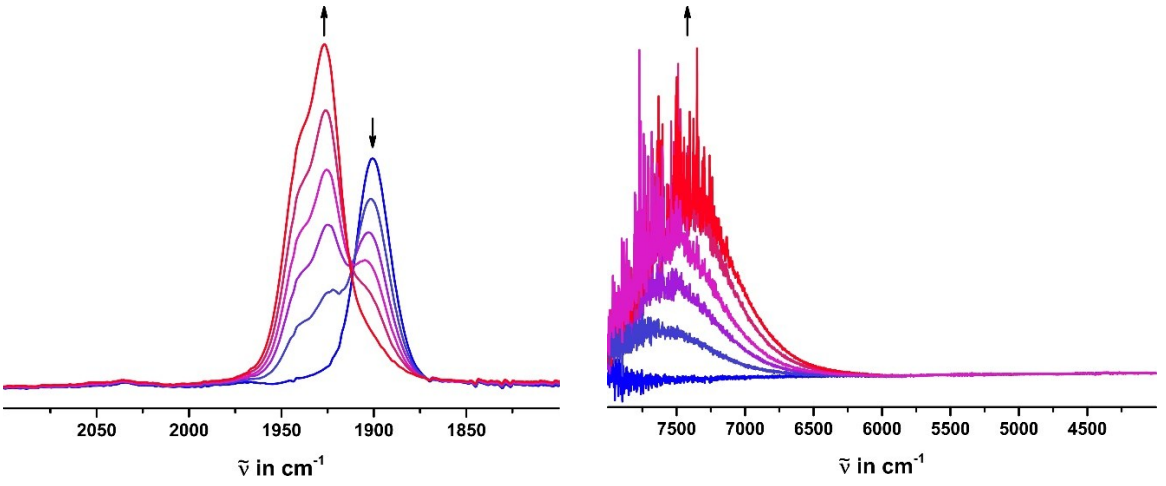

Figure 24. Changes in the IR spectra of **1-H** on oxidation to **1-H**$^{2+}$ (CH_2Cl_2/NBu_4PF_6 at r. t.).

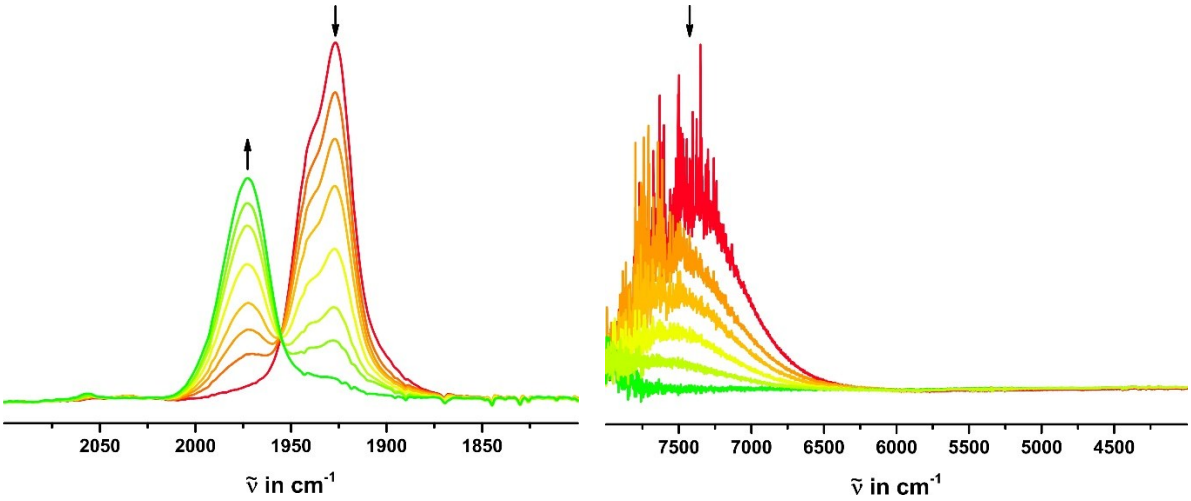

Figure 25. Changes in the IR spectra on further oxidation of **1-H**$^{2+}$ to **1-H**$^{4+}$ (CH_2Cl_2/NBu_4PF_6 at r. t.).

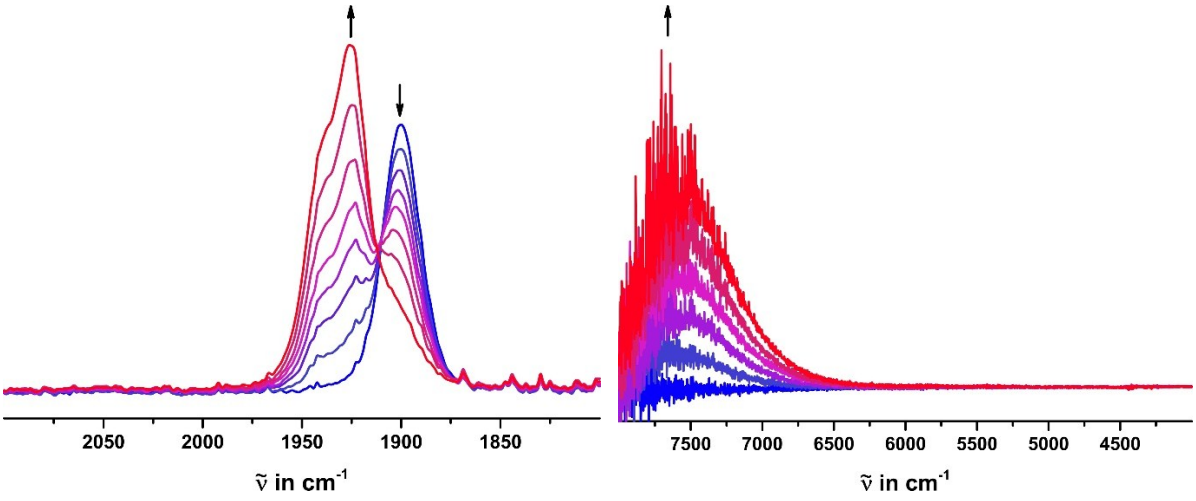

Figure 26. Changes in the IR spectra of **1-OMe** on oxidation to **1-OMe**$^{2+}$ (CH_2Cl_2/NBu_4PF_6 at r. t.).

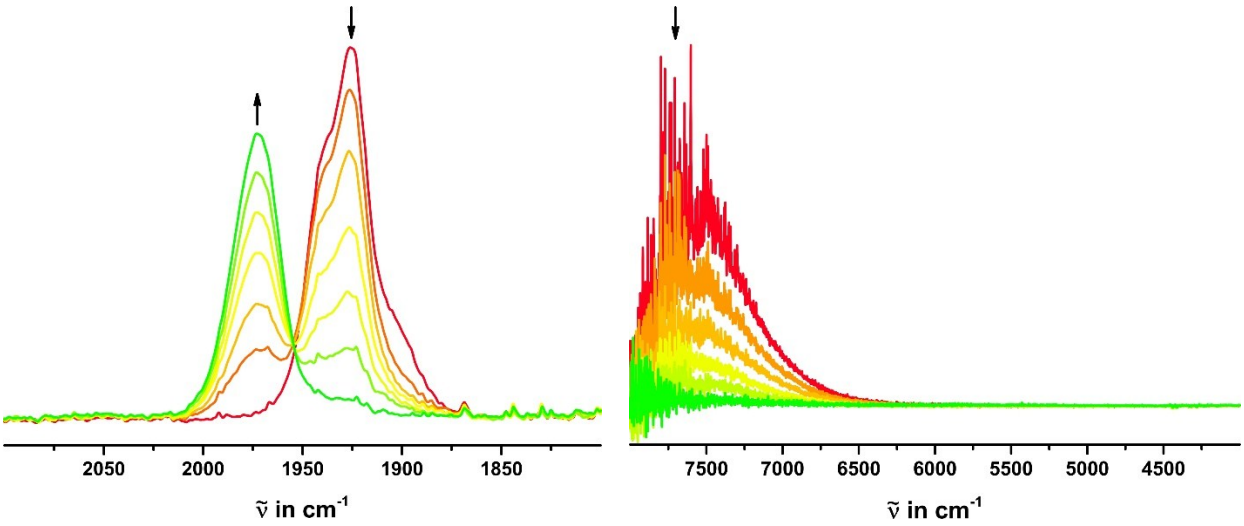

Figure 27. Changes in the IR spectra on further oxidation of **1-OMe**$^{2+}$ to **1-OMe**$^{4+}$ (CH_2Cl_2/NBu_4PF_6 at r. t.).

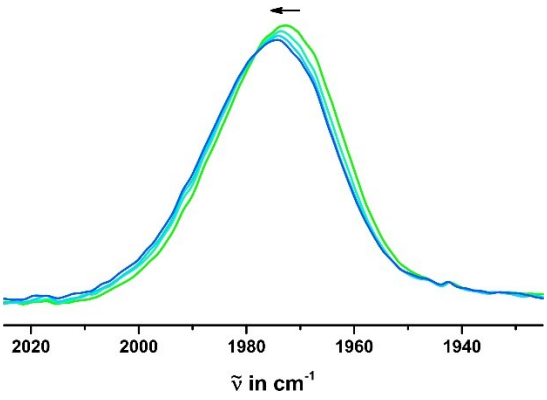

Figure 28. Changes in the ν(CO) region on further oxidation of **1-OMe**$^{4+}$ to **1-OMe**$^{6+}$ (CH_2Cl_2/NBu_4PF_6 at r. t.).

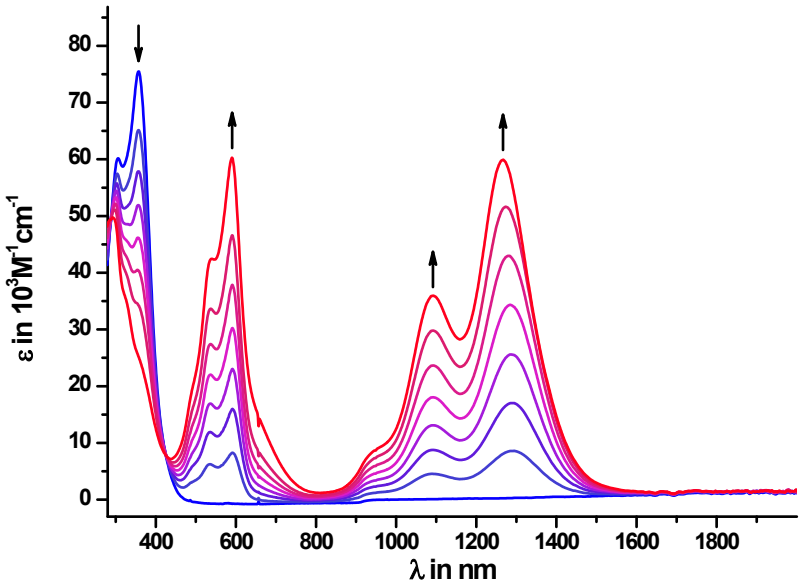

Figure 29. Changes in the UV/Vis/NIR spectrum of **1-H** on oxidation to **1-H**$^{2+}$ (CH_2Cl_2/NBu_4PF_6 at r. t.).

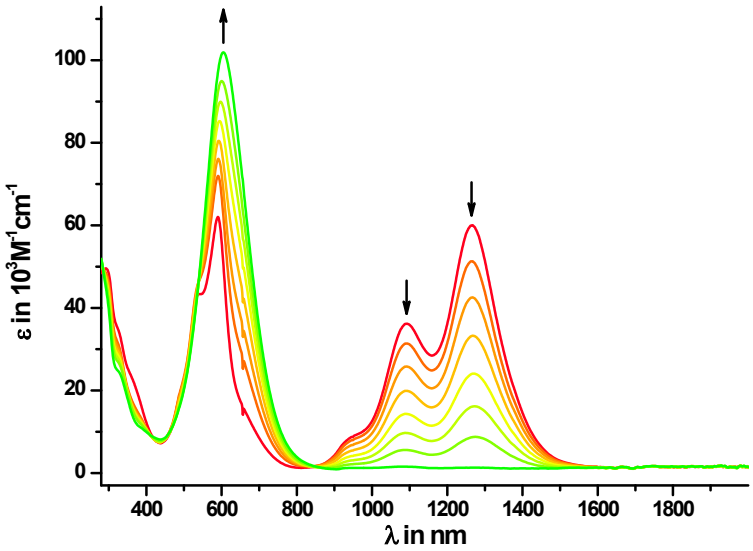

Figure 30. Changes in the UV/Vis/NIR spectrum of **1-H**$^{2+}$ on oxidation to **1-H**$^{4+}$ (CH_2Cl_2/NBu_4PF_6 at r. t.).

References

1. H. Werner, M. A. Esteruelas and H. Otto, *Organometallics*, 1986, **5**, 2295.
2. J. Maurer, B. Sarkar, B. Schwederski, W. Kaim, R. F. Winter and S. Záliš, *Organometallics*, 2006, **25**, 3701-3712.
3. F. Monnier and M. Taillefer, *Angew. Chem. Int. Ed. Engl.*, 2009, **48**, 6954-6971.
4. H. Murata and P. M. Lahti, *J. Org. Chem.*, 2007, **72**, 4974-4977.
5. M. Krejcik, M. Danek and F. Hartl, *J. Electroanal. Chem.*, 1991, **317**, 179-187.
6. G. M. Sheldrick, SHELX-97, Program for Crystal Structure Solution and Refinement, Universität Göttingen, 1997.